

## Meta-Learning Empowered Receiver Design for MIMO-OFDM System Under HPA Nonlinearity

Zishen Liu, Nan Wu<sup>ID</sup>, Senior Member, IEEE,  
 Dongxuan He<sup>ID</sup>, Member, IEEE,  
 Weijie Yuan<sup>ID</sup>, Senior Member, IEEE,  
 and Chau Yuen<sup>ID</sup>, Fellow, IEEE

**Abstract**—In this correspondence, a meta-learning empowered detector is proposed for multiple-input multiple-output orthogonal frequency-division multiplexing (MIMO-OFDM) systems under nonlinear distortions of high power amplifier (HPA). By utilizing the residual connection that directly transmits the data flow into the last layer, a deep neural network (DNN)-aided detector is proposed to blindly compensate the nonlinear distortions and denoise. By introducing learnable parameters into nonlinear models, a model-driven compensator is proposed to further improve nonlinearity compensation without the aid of specific HPA characteristic parameters. To enhance the adaptivity of our proposed compensator, a meta-learning empowered scheme with offline training and fast online adaptation is developed by fully leveraging the supervised information from pilots. Simulation results demonstrate that our proposed detector can achieve satisfactory performance in MIMO-OFDM systems under HPA nonlinearity, while showing the superior online adaptivity with few pilots and gradient updates.

**Index Terms**—Meta-learning, high power amplifiers, model-driven detector, nonlinear distortion, MIMO-OFDM.

### I. INTRODUCTION

Multiple-input multiple-output orthogonal frequency-division multiplexing (MIMO-OFDM) has shown great potential in providing high spectral efficiency, thus making it a key technology in the upcoming sixth-generation (6G) wireless communication [1]. However, due to the large peak-to-average power ratio (PAPR) of OFDM modulation, high power amplifiers (HPAs) in MIMO-OFDM transmitters are easy to operate near the saturation point, leading to the severe nonlinear distortions [2]. Therefore, it is greatly challenging to achieve acceptable detection performance in MIMO-OFDM systems under HPA nonlinearity.

To tackle this challenge, various works focus on alleviating the impact of nonlinear distortions [3], [4], [5], [6]. Particularly, nonlinear

Received 12 March 2025; revised 14 June 2025; accepted 15 July 2025. Date of publication 18 July 2025; date of current version 19 January 2026. This work was supported in part by the National Key Research and Development Program of China under Grant 2024YFE0200404 and Grant 2021YFB2900600, in part by the National Natural Science Foundation of China under Grant 61971041, Grant 62371045, Grant 62301060, and Grant 62471208, and in part by Guangdong Provincial Natural Science Foundation under Grant 2024A151510098. The review of this article was coordinated by Prof. Hayssam Dahrourj. (*Corresponding authors:* Nan Wu; Dongxuan He.)

Zishen Liu, Nan Wu, and Dongxuan He are with the School of Information and Electronics, Beijing Institute of Technology, Beijing 100081, China (e-mail: zishen\_liu@bit.edu.cn; wunan@bit.edu.cn; dongxuan\_he@bit.edu.cn).

Weijie Yuan is with the School of System Design and Intelligent Manufacturing and the Shenzhen Key Laboratory of Robotics and Computer Vision, Southern University of Science and Technology, Shenzhen 518055, China (e-mail: yuanwj@sustech.edu.cn).

Chau Yuen is with the School of Electrical and Electronics Engineering, Nanyang Technological University, Singapore 639798 (e-mail: chau.yuen@ntu.edu.sg).

Digital Object Identifier 10.1109/TVT.2025.3590459

compensation at the receiver side, has gained widespread attention in MIMO-OFDM uplink systems due to the sufficient hardware and computational resources in base station (BS) [4], [5], [6]. In [4], an hybrid analog-digital iterative equalizer with a feedback loop was developed to jointly mitigate the multiuser interference (MUI) and nonlinear distortions. In [5], A unified HPA representation-based equalization technique was developed for nonlinear OFDM signal detection. In [6], a hybrid message passing method was proposed to achieve joint channel estimation and soft symbol decoding under nonlinear distortions. However, these methods are typically impractical due to the reliance on perfectly known transmitters' HPA characteristics. As such, how to effectively compensate nonlinear distortions without HPA features is still challenging in uplink MIMO-OFDM systems.

Benefiting from its excellent ability in extracting implicit features, deep learning (DL) can be widely utilized to compensate nonlinear distortions [7], [8], [9]. For instance, model aided DL-based receivers were developed to find the nonlinear mappings without HPA information [7], [8]. However, such DL-based detectors show poor adaptivity when online nonlinearity differs from that in the training data. To address this issue, slow time (ST) training sequence was introduced in transmission frame to perform online retraining of learnable modules [9]. Nevertheless, significant overhead is required, especially in the high-mobility environment, where the user transmission power selection depends on the distance from the BS, leading to frequent changes of HPA nonlinear effects.

Inspired by the above background, a meta-learning empowered detector for MIMO-OFDM uplink systems in the presence of HPA nonlinearity is proposed in this correspondence. Our main contributions are summarized as follows: 1) By utilizing the deep residual structure and model-driven deep unfolding approach, a deep learning-aided nonlinear compensation framework is proposed to perform hybrid time-frequency equalization without HPA characteristics at receiver side. 2) Leveraging the supervised information from pilots, a meta-learning empowered scheme with offline training and online few-shot adaptation is developed to enhance compensation adaptivity while maintaining satisfactory spatial efficiency. Simulation results demonstrate that our proposed meta-learning empowered compensation can achieve good performance in MIMO-OFDM systems under nonlinear distortions, while showing the superior online adaptive ability with few pilots and gradient updates.

### II. SYSTEM MODEL

We consider a MIMO-OFDM uplink system where a BS equipped with  $N_r$  receive antennas serves  $\widetilde{N}_t$  single-antenna users, as demonstrated in Fig. 1. Specifically, the  $M$ -quadrature amplitude modulation (QAM) complex symbols in the frequency domain are mapped to an OFDM symbol with  $N_c$  subcarriers. Accordingly, a  $N_c$ -point inverse fast fourier transform (IFFT) is employed to transform the transmitted symbols from frequency domain, i.e.,  $\mathbf{X}[k] \in \mathbb{C}^{N_t \times 1}$ , to the time domain, given as

$$x_i[n] = \frac{1}{\sqrt{N_c}} \sum_{k=0}^{N_c-1} x_i[k] e^{\frac{j2\pi knT}{T_s}}, \quad 0 \leq n \leq N_c, \quad (1)$$

where  $T$  and  $T_s$  are the sampling period and OFDM symbol duration, respectively. To address ISI, a cyclic prefix (CP) is added to every OFDM symbol, given as  $x_i^{(cp)} = [x_i[N_c - L_{cp} + 1], \dots, x_i[N_c], \mathbf{x}_i^T]^T \in$

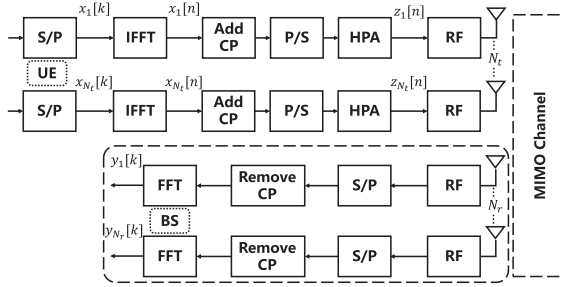


Fig. 1. Block diagram of MIMO-OFDM uplink system.

$\mathbb{C}^{(N_c+L_{cp}) \times 1}$ , where  $L_{cp} \geq L_h - 1$  and  $L_h$  is the maximum length of the channel impulse response (CIR). Then, the transmitted signal is distorted by the nonlinear HPA, the effect of which can be characterized by the Rapp model [3], [4], given by

$$z = g(x) = x \left( 1 + \left( \frac{|x|}{A_{\text{sat}}} \right)^{2\delta} \right)^{-\frac{1}{2\delta}}, \quad (2)$$

where  $A_{\text{sat}}$  is the saturated output of HPA and  $\delta$  is the smooth factor. According to [10], the distortion depends on the clipping level defined by  $\gamma = 10 \log(A_{\text{sat}}^2/P_x)$ , where  $P_x$  is the average input power of HPA.

After removing CP, the received signal  $\mathbf{Y}[k] \in \mathbb{C}^{N_r \times 1}$  in frequency domain can be expressed as

$$\mathbf{Y}[k] = \mathbf{H}[k]\mathbf{Z}[k] + \mathbf{N}[k], \quad (3)$$

where  $\mathbf{H}[k] \in \mathbb{C}^{N_r \times N_t}$  is channel matrix of the  $k$ -th subcarrier, derived by applying  $N_c$ -point fast fourier transform (FFT) to the CIR.  $\mathbf{Z}[k] \in \mathbb{C}^{N_t \times 1}$  is the nonlinear distorted transmitted signal in frequency domain, whose element is given by

$$z_i[k] = \frac{1}{\sqrt{N_c}} \sum_{n=0}^{N_c-1} g(x_i[n]) e^{-j2\pi knT_s}, \quad 0 \leq k \leq N_c. \quad (4)$$

$\mathbf{N}[k] \in \mathbb{C}^{N_r \times 1}$  denotes additive white Gaussian noise (AWGN) of the  $k$ -th subcarrier with zero mean and element-wise variance  $\sigma^2$ .

In this work, we suppose  $\mathbf{H}[k]$  can be accurately estimated at the receiver side [9], while the nonlinearity of HPAs is unavailable at the receiver side. Consequently, the MUI caused by MIMO channels can be mitigated by zero forcing (ZF) detection in frequency domain, given by

$$\hat{\mathbf{Z}}[k] = (\mathbf{H}[k])^\dagger \mathbf{Y}[k] = \mathbf{Z}[k] + \bar{\mathbf{N}}[k], \quad (5)$$

where  $(\mathbf{H}[k])^\dagger$  is the pseudoinverse of  $\mathbf{H}[k]$ , i.e.,  $(\mathbf{H}[k])^\dagger = ((\mathbf{H}[k]^H \mathbf{H}[k])^{-1} (\mathbf{H}[k])^H)$ , and  $\bar{\mathbf{N}}[k] = (\mathbf{H}[k])^\dagger \mathbf{N}[k]$ .

### III. DEEP LEARNING-AIDED NONLINEAR COMPENSATION

In this section, a deep learning-aided nonlinear compensation framework is developed to perform hybrid time-frequency equalization, where DNN-aided compensation and model-driven iterative LS-based compensation are proposed to blindly compensate HPA nonlinearity and further improve compensation performance by integrating learnable HPA nonlinear features, respectively.

#### A. Blind DNN-Aided Nonlinear Compensation and Denoising

To eliminate the impacts of nonlinear distortions and enhanced noise without nonlinear characteristics at the receiver side, a DNN-aided

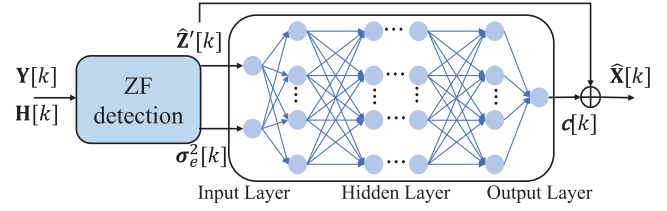


Fig. 2. The proposed blind DNN-aided compensator.

module is proposed to blindly compensate HPA nonlinearity and de-noise in frequency domain, as illustrated in Fig. 2.

In particular, the output of ZF detection and the enhanced noise variance are selected as the inputs of DNN, given as

$$\boldsymbol{\mu}_0[k] = [\hat{\mathbf{Z}}'[k], \sigma_e^2[k]]^T, \quad (6)$$

where  $\hat{\mathbf{Z}}'[k] = [\Re(\hat{\mathbf{Z}}[k])^T \Im(\hat{\mathbf{Z}}[k])^T]^T$  is the concatenation of the real and imaginary parts of  $\hat{\mathbf{Z}}[k]$ .  $\Re(\cdot)$  and  $\Im(\cdot)$  are the options that extract real and imag part, respectively.  $\sigma_e^2[k] \in \mathbb{R}^{2N_t \times 1}$  is the noise variance feature to tackle the enhanced noise, given as

$$\sigma_e^2[k] = \left[ \left( \frac{\sigma^2}{2} |(\mathbf{H}[k])^\dagger|^2 \mathbf{1}_{N_r \times 1} \right)^T \left( \frac{\sigma^2}{2} |(\mathbf{H}[k])^\dagger|^2 \mathbf{1}_{N_r \times 1} \right)^T \right]^T, \quad (7)$$

where  $\mathbf{1}_{N_r \times 1}$  denotes the all-one vector of size  $N_r \times 1$ .

Moreover, the DNN module employs a multiple layer perception (MLP) with  $L_n$  layers, where the output of the  $i$ -th layer can be formulated as  $\boldsymbol{\mu}_i[k] = f(\mathbf{W}_i \boldsymbol{\mu}_{i-1}[k] + \mathbf{b}_i)$ .  $\mathbf{W}_i$  and  $\mathbf{b}_i$  denote the weight matrix and bias of the  $i$ -th layer, respectively,  $f(\cdot)$  denotes the activation function. More specifically, identity function  $f(x) = x$  is selected as the activation function of the output layer, while ReLU is employed as that of the hidden layer to capture nonlinearity.

To accelerate the DNN training and improve compensation performance, residual connection that directly transmits the data flow into the last layer, is employed by adding the DNN input  $\hat{\mathbf{Z}}'[k]$  with the output  $\mathbf{c}[k]$  [11], as presented in Fig. 2. Then, the estimation of transmitted symbols, i.e.,  $\hat{\mathbf{X}}[k]$ , is obtained by transferring the summation of  $\hat{\mathbf{Z}}'[k]$  and  $\mathbf{c}[k]$  to the complex-valued form.

#### B. Model-Driven Iterative LS-Based Compensation

Although the DNN-aided compensator can alleviate the nonlinear distortions of HPA, its performance is limited since the ISI in frequency domain is difficult to be effectively eliminated. To eliminate such ISI, the domain knowledge of HPAs is usually employed to further perform equalization in time domain. However, the methods in [5] are impractical owing to the difficulty of obtaining HPA characteristics, e.g., clipping level  $\gamma$  and smoother factor  $\delta$ , at the BS.

Motivated by this, a model-driven iterative least square (LS) compensator, named IterLSNet, is proposed by introducing the learnable parameters into the iterative LS framework to leverage available models without HPA features, as demonstrated in Fig. 3. With the IFFT of output of DNN-aided compensator as the initialization, an approximate HPA transfer vector  $\lambda^l \in \mathbb{R}^{N_t \times N_c}$  is derived according to (2), given as

$$\lambda_i^l[n] = R(\hat{x}_i^{l-1}[n]; \gamma', \delta') = \left( 1 + \left( \frac{|\hat{x}_i^{l-1}[n]|}{A'_{\text{sat}}} \right)^{2\delta'} \right)^{-\frac{1}{2\delta'}}, \quad (8)$$

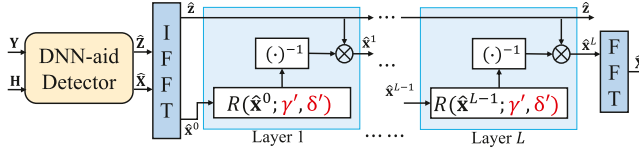


Fig. 3. The proposed model-driven IterLSNet.

where  $\gamma'$  and  $\delta'$  are learnable parameters.  $A'_{\text{sat}}$  is obtained by  $\gamma' = 10 \log(A'^2_{\text{sat}}/P_{\hat{x}})$ . Then, the symbol estimation is updated by LS estimation, given by

$$\hat{\mathbf{x}}^l = \frac{1}{\lambda^l} \odot \hat{\mathbf{z}}, \quad (9)$$

where  $\frac{1}{\lambda^l}$  is the element-wise inverse of  $\lambda^l$ ,  $\odot$  denotes the Hadamard product.

After  $L$  layers' processing, the symbol estimation  $\hat{\mathbf{X}}^L$  can be obtained by the FFT of  $\hat{\mathbf{x}}^L$ .

To optimize learnable parameters, a mean square error (MSE) loss function is employed for our proposed compensation schemes, given as

$$\mathcal{L}(\boldsymbol{\theta}_m) = \frac{1}{BN_c N_t} \sum_{b=1}^B \sum_{k=1}^{N_c} \|\hat{\mathbf{X}}[k] - \mathbf{X}[k]\|_2^2, m \in \{1, 2\} \quad (10)$$

where  $B$  is the number of OFDM symbols per frame,  $\boldsymbol{\theta}_m$  is the learnable parameter set, which can be  $\boldsymbol{\theta}_1 = [\mathbf{W}_1, \mathbf{b}_1, \dots, \mathbf{W}_{L_n}, \mathbf{b}_{L_n}]$  and  $\boldsymbol{\theta}_2 = [\boldsymbol{\theta}_1, \gamma', \delta']$  for DNN and IterLSNet, respectively.

#### IV. META-LEARNING EMPOWERED ONLINE ADAPTATION

Due to the integration of domain knowledge, IterLSNet with the unfolding structure highly relies on the specific HPA realizations. However, users tend to select different transmission power with the distance from BS to resist path loss, resulting in the change of HPA operating point. In dynamic environment, such changes would be extremely frequent, and mismatches between trained IterLSNet and the nonlinear distortions to be compensated would significantly deteriorate the detection performance. ST sequences are typically employed in frame structure to perform online parameter retraining [9]. However, significant system overhead would be introduced by such a design, which cannot be ignored, particularly in high-mobility scenarios.

To achieve effective online adaptation, a meta-learning empowered approach is proposed in this section to find initial parameters that are sensitive to changes of the HPA nonlinear effect and reuse the supervised information from pilots to achieve online fine-tuning. In particular, our proposed approach includes two stages, namely the offline meta-training and online few-shot adaptation.

##### A. Offline Meta-Training

A model-agnostic meta-learning (MAML) method is adopted to obtain the inductive bias for fast adaptation toward any nonlinear characteristics during online learning stage. Consequently, the objective of the meta-training is given by

$$\min_{\boldsymbol{\theta}_2} \sum_{\mathcal{T}(t) \sim Q} \mathcal{L}_{\mathbb{D}(t)}(\boldsymbol{\theta}'_2(t)), \quad (11)$$

where  $\mathcal{T}(t)$  represents different HPA characteristics drawn from the distribution  $Q$  with a dataset  $\mathbb{D}(t)$ , and  $\boldsymbol{\theta}'_2(t)$  is the adaptation with the gradient updates by  $\boldsymbol{\theta}_2$  based on certain HPA characteristic, given as

$$\boldsymbol{\theta}'_2(t) = \boldsymbol{\theta}_2 - \alpha \nabla_{\boldsymbol{\theta}_2} \mathcal{L}_{\mathbb{D}(t)}(\boldsymbol{\theta}_2). \quad (12)$$

To obtain  $\boldsymbol{\theta}_2$  that optimizes (11), a training data preparation is employed to demonstrate the adaptation in (12). Given the compensation scheme in Section III, the features in (6) and the true symbols are utilized as input data and corresponding labels, respectively.  $N_{\text{tr}}$  meta-training tasks are drawn from  $Q$  and denoted as  $\{\mathcal{T}_{\text{tr}}(t)\}_{t=1}^{N_{\text{tr}}}$ . For task  $\mathcal{T}_{\text{tr}}(t)$ , the data set  $\mathbb{D}_{\text{tr}}(t)$  is split into the support set  $\mathbb{D}_s(t)$  and the query set  $\mathbb{D}_q(t)$ .

Based on the generated datasets, the objective in (11) is achieved by two training steps, namely inner-task and cross-task updates. At first, the meta-learner updates inner-task parameters  $\varphi$  by utilizing the support set  $\mathbb{D}_s(t)$  with the initialization of global parameters  $\boldsymbol{\theta}_2$ , i.e.,  $\varphi_0(t) = \boldsymbol{\theta}_2$ . By iteratively calculating  $\mathcal{L}_{\mathbb{D}_s(t)}(\varphi_{l_o-1}(t))$  using (10), inner-task parameters are updated through the stochastic gradient descent (SGD) method [12], denoted as

$$\varphi_{l_o}(t) = \varphi_{l_o-1}(t) - \alpha \nabla_{\varphi_{l_o-1}(t)} \mathcal{L}_{\mathbb{D}_s(t)}(\varphi_{l_o-1}(t)), \quad (13)$$

where  $\alpha$  represents the inner-task learning rate.

After  $L_{\text{in}}$  inner iterations, the cross-task update is executed to optimize the global network parameter  $\boldsymbol{\theta}_2$ . Specifically, the loss on the query set is computed utilizing the network parameters after inner update, denoted as  $\mathcal{L}_{\mathbb{D}_q(t)}(\varphi_L(t))$ . Then, the losses calculated from different tasks are accumulated and subsequently utilized to update by the adaptive moment estimation (Adam) optimizer [13], given as<sup>1</sup>

$$\begin{aligned} \boldsymbol{\theta}_2 &\leftarrow \boldsymbol{\theta}_2 + \beta \cdot \text{Adam}(\nabla_{\boldsymbol{\theta}_2} \bar{\mathcal{L}}, \boldsymbol{\theta}_2) \\ &= \boldsymbol{\theta}_2 + \beta \cdot \text{Adam}\left(\frac{1}{N_{\text{tr}}} \sum_{t=1}^{N_{\text{tr}}} \mathbf{J}_{\theta}(\varphi_L(t)) \nabla_{\varphi_L(t)} \mathcal{L}_{\mathbb{D}_q(t)}(\varphi_L(t)), \boldsymbol{\theta}_2\right) \\ &\approx \boldsymbol{\theta}_2 + \beta \cdot \text{Adam}(\nabla_{\boldsymbol{\theta}_2} \bar{\mathcal{L}}, \boldsymbol{\theta}_2), \end{aligned} \quad (14)$$

where  $\bar{\mathcal{L}} = \frac{1}{N_{\text{tr}}} \sum_{t=1}^{N_{\text{tr}}} \mathcal{L}_{\mathbb{D}_q(t)}(\varphi_L(t))$ ,  $\mathbf{J}_{\theta}(\cdot)$  represents the Jacobian operation, and  $\beta$  is the cross-task learning rate.

According to (13) and (14), the BS can perform inner-task and cross-task updates iteratively with  $N_{\text{epoch}}$  epochs, then train a model with the most adaptive parameters  $\boldsymbol{\theta}_{2,\text{off}}$  among various tasks, i.e., different HPA nonlinearity.

##### B. Online Few-Shot Adaptation

During online training stage, the BS performs fine-tuning with  $\boldsymbol{\theta}_{2,\text{off}}$  outputted in meta-training stage to quickly adapt to current HPA characteristics. By fully using the natural supervised information of pilots in a OFDM frame, an online few-shot adaptation scheme is proposed to remain spectral efficiency.

With  $\boldsymbol{\theta}_{2,\text{off}}$  as the initialization, online training is performed through SGD to adapt the learnable parameters to the optimal for current HPA nonlinearity, given by

$$\boldsymbol{\theta}_{2,l_a} = \boldsymbol{\theta}_{2,l_a-1} - \alpha \nabla_{\boldsymbol{\theta}_2} \mathcal{L}_{\mathbb{D}_p}(\boldsymbol{\theta}_{2,l_a-1}), \quad (15)$$

where  $\mathcal{L}_{\mathbb{D}_p}$  is the loss computed by (10) based on pilots  $\mathbb{D}_p$ . After finishing fine-tuning with  $L_{\text{ft}}$  gradient steps, the data symbols can be detected using the optimal parameters  $\boldsymbol{\theta}_{2,\text{opt}}$ , achieving superior performance under the current status of nonlinearity.

The details of our proposed meta-learning empowered nonlinearity compensation are summarized in **Algorithm 1**.

<sup>1</sup>According to [17], in the transformation from  $\nabla_{\boldsymbol{\theta}}$  to  $\nabla_{\varphi_L}$ , second-order and higher-order derivatives maximize the inner-task generation, while first-order derivative maximizes the inner products between the gradients computed on different tasks. Thus, second-derivative terms are ignored, as they has only a negligible impact on performance [14].

TABLE I  
IMPLEMENT PARAMETERS

| Parameter   | Value   |
|---|---|
| BS antenna number $N_r$                           | 16  |
| User number $N_t$                                 | 8   |
| QAM order $\bar{M}$                               | 16  |
| OFDM symbol number per frame $B$                  | 32  |
| Pilot length per frame $N_p$                      | 1   |
| Subcarrier number per OFDM symbol $N_c$           | 128   |
| Channel Length $L_h$                              | 6   |
| Number of neurons $N_{ne}$                        | 64  |
| DNN layer width                                   | $(N_{ne}, \frac{N_{ne}}{2}, \frac{N_{ne}}{4}, 1)$ |
| IterLSNet unfolding layer number $L$              | 2   |
| Offline and online update number $L_{in}, L_{ft}$ | 5   |
| Task number $N_{tr}$                              | 256   |
| Inner-task learning rate $\alpha$                 | 0.04  |
| Cross-task learning rate $\beta$                  | 0.0002  |
| Epochs for cross-task update $N_{epoch}$          | 60000   |

**Algorithm 1:** Meta-Learning Empowered Nonlinear Compensation.

```

Input:  $\{\mathcal{T}_{tr}(t)\}_{t=1}^{N_{tr}}$ ,  $\alpha$ ,  $\beta$ ,  $N_{epoch}$ ,  $L_{in}$ ,  $L_{ft}$ 
Output: Online data symbol detection results

// Offline Meta-Training:
1 Randomly initialize the learnable parameters  $\theta_2$ ;
2 for  $j = 1$  to  $N_{epoch}$  do
3   Randomly sample data from  $\{\mathcal{T}_{tr}(t)\}_{t=1}^{N_{tr}}$  to generate
       $\{\mathbb{D}_{tr}(t)\}_{t=1}^{N_{tr}}$ ;
4   Split  $\{\mathbb{D}_{tr}(t)\}_{t=1}^{N_{tr}}$  as  $\{\mathbb{D}_s(t)\}_{t=1}^{N_{tr}}$  and  $\{\mathbb{D}_q(t)\}_{t=1}^{N_{tr}}$ ;
5   for  $t = 1$  to  $N_r$  do
6     for  $l_o = 1$  to  $L_{in}$  do
7       Update  $\varphi_{l_o}(t)$  using (13) with  $\mathbb{D}_s(t)$ ;
8     Update  $\theta_2$  using (14) with  $\mathbb{D}_q(t)$ ;
9
// Online Few-Shot Adaptation:
10 Generate  $\mathbb{D}_p$  according to receive signal;
11 Load the pre-trained parameters  $\theta_{2,off}$ ;
12 for  $l_a = 1$  to  $L_{ft}$  do
13   Fine-tune the learnable parameters using (15) with  $\mathbb{D}_p$ ;
14 Perform data detection based on receive signal and  $\theta_{2,opt}$ ;

```

## V. SIMULATION RESULTS

In this section, numerical results are presented to demonstrate the superiority of proposed detectors for MIMO-OFDM systems under nonlinear distortions of HPA, where ZF, LMMSE, Bussgang [15], ARVTDNN [9], and SPs-ILSE [5] methods are selected as comparison. Moreover, to verify the effectiveness of our proposed meta-learning empowered IterLSNet (meta-IterLSNet), other learning schemes for proposed IterLSNet are introduced for comparison, as listed below:

- S1) Optimal IterLSNet: This scheme provides as a performance upper bound obtained by using consistent HPA characteristics in both training and testing datasets.
- S2) Non-adaptive (NA)-IterLSNet: This scheme shows the result obtained by training the IterLSNet with HPA characteristics that differs from that in the testing dataset.
- S3) Joint training (JT)-IterLSNet: This scheme shows the result obtained by training the IterLSNet using all available HPA characteristics without adaptation [16].

Throughout the experiments, we assume the system parameters of our proposed detectors are set as Table I. For comparison, all learning

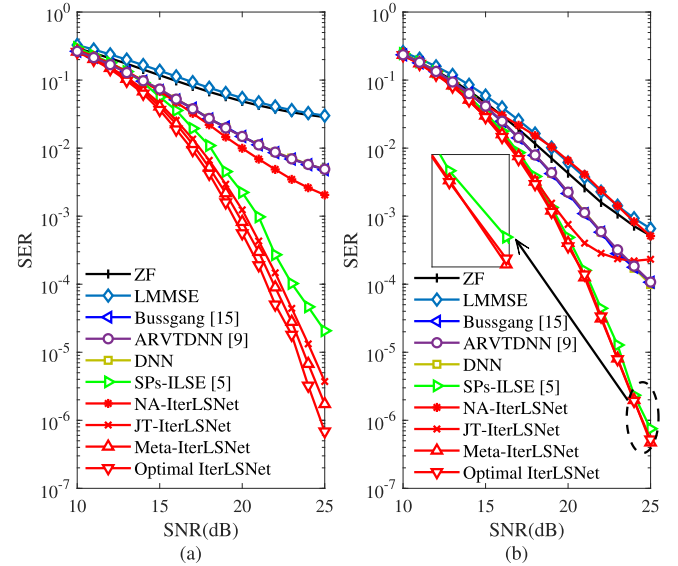


Fig. 4. SER performance comparison under different distortions of (a)  $\gamma = 3$  dB,  $\delta = 2$  and (b)  $\gamma = 5$  dB,  $\delta = 2$ .

schemes adopt similar parameters, while S1-S3 undergo a training process of 100 epochs with  $10^5$  samples, where Adam optimizer is used with a learning rate of  $10^{-3}$  [18], [19]. All simulations are executed on a desktop with GPU NVIDIA GeForce RTX 4090 and Pytorch 2.0.0 environment.

To show the superiority of our proposed detectors, Fig. 4 illustrates SER performance of ZF, LMMSE, Bussgang, ARVTDNN, SPs-ILSE, DNN-aided detector, and IterLSNet with four learning schemes. Under different clipping levels, the proposed blind DNN-aided detector performs similarly to Bussgang, but without requiring reference signals, and outperforms both ZF and LMMSE detectors, which benefits from its effective compensation for nonlinear distortions and noise.<sup>2</sup> Moreover, it can be verified that our proposed meta-IterLSNet outperforms the SPs-ILSE with perfect known HPA nonlinear features and achieve similar performance of optimal IterLSNet by online adaptation, showing great robustness to changes of HPA nonlinear effects. For instance, in Fig. 4(a), when  $\gamma = 3$  dB, our proposed meta-IterLSNet outperforms JT-IterLSNet<sup>3</sup> with about 1dB gain at  $SER = 10^{-5}$ , and outperforms SPs-ILSE with about 2dB at  $SER = 10^{-4}$ .

To show the effectiveness of our proposed meta-learning empowered online few-shot adaptation for IterLSNet, Fig. 5 demonstrates the SER changes with online gradient update steps using pilots, where all schemes adopt the SGD optimizer with learning rate of 0.04 for comparison. It can be seen that our proposed meta-learning empowered online few-shot adaptation can fast update to the optimal within around 4 updating gradient steps. By contrast, the NA-IterLSNet cannot reach convergence within 20 steps, while the trained model of JT-IterLSNet is not sensitive to the few-shot supervised information. Additionally, performance gaps between them and meta-learning remain significant.

<sup>2</sup>By comparing the performance of LMMSE and ZF, it can be seen that, simply considering denoising without nonlinearity compensation cannot improve the detection performance.

<sup>3</sup>Since there may not be a single trained model that guarantees a desirable average performance on all HPA characteristics and SNR conditions [16], JT-IterLSNet fails to improve nonlinearity compensation performance under non-serious nonlinear distortions, thus leading to a SER floor in high SNR regimes in Fig. 4(b).

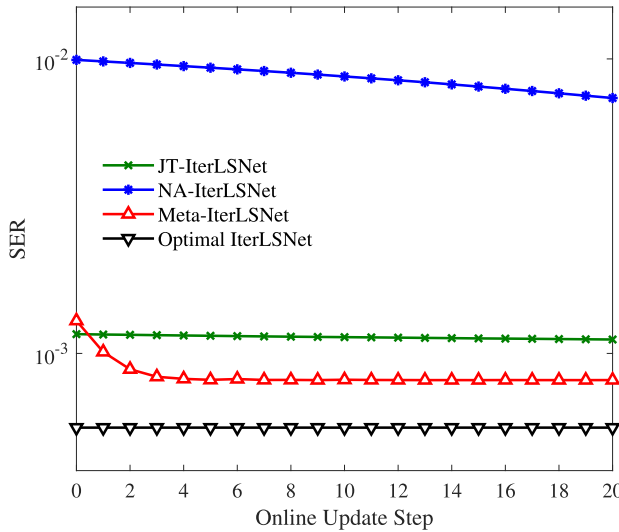


Fig. 5. Online adaptation comparison between different learning schemes with  $\gamma = 3$  dB and  $\delta = 2$  at SNR = 20 dB.

For instance, our proposed meta-IterLSNet can achieve an SER of less than  $10^{-3}$  after completing 3 online update steps, while the JT-IterLSNet and NA-IterLSNet can only achieve an SER greater than  $10^{-3}$  within 20 training steps.

Moreover, the computational complexity of two proposed compensators is on the order of  $O(\frac{5}{4}N_t N_c N_{ne}^2)$  and  $O(N_t N_c (\frac{5}{4}N_{ne}^2 + 5L + 2 \log_2 N_c))$  for per OFDM symbol transmission, respectively.<sup>4</sup> For the DNN-aided detector, the number of real-valued multiplications of the four-layer DNN is  $2N_t N_c (2N_{ne} + \frac{N_{ne}^2}{2} + \frac{N_{ne}^2}{8} + \frac{N_{ne}}{4})$ . Therefore, the complexity order is  $O(\frac{5}{4}N_t N_c N_{ne}^2)$ . For the IterLSNet, the approximate HPA transfer vector calculation in (8) and the LS estimation in (9) only contain element-wise exponentiation and multiplications, while the IFFT and FFT operations are employed for the input and output. Accordingly, the number of real-valued multiplications of the model-driven part is  $10N_t N_c L + 2N_t N_c \log_2 N_c$ . Thus, the whole computational complexity order of IterLSNet is  $O(N_t N_c (\frac{5}{4}N_{ne}^2 + 10L + 2 \log_2 N_c))$ .

## VI. CONCLUSION

In this correspondence, adaptive compensation schemes for HPA nonlinearity were developed for MIMO-OFDM uplink systems. In particular, a DNN-aided compensator was firstly proposed to blindly compensate the nonlinear distortions and denoise through the residual connection. With the output of the DNN-aided compensator as initialization, a model-driven IterLSNet was proposed to further equalize the distortions by leveraging HPA models in the absence of HPA characteristics. To enhance the adaptive ability of proposed compensators, a MAML-based fast adaptation approach was further developed to

<sup>4</sup>Since ZF detection is utilized in every receiver and the training of learnable components can be realized offline, only the computational complexity of the online nonlinear compensation is analyzed.

quickly adjust to the optimal under various HPA characteristics with few pilots and gradient updates. Simulation results validated the superiority of our proposed compensation schemes and demonstrated the effectiveness of meta-learning empowered online few-shot adaptation compared to other learning schemes.

## REFERENCES

- [1] K. B. Letaief, W. Chen, Y. Shi, J. Zhang, and Y.-J. A. Zhang, "The roadmap to 6G: AI empowered wireless networks," *IEEE Commun. Mag.*, vol. 57, no. 8, pp. 84–90, Aug. 2019.
- [2] Y. Huleihel and H. H. Permuter, "Low PAPR MIMO-OFDM design based on convolutional autoencoder," *IEEE Trans. Commun.*, vol. 72, no. 5, pp. 2779–2792, May 2024.
- [3] J. Joung, C. K. Ho, K. Adachi, and S. Sun, "A survey on power amplifier-centric techniques for spectrum and energy-efficient wireless communications," *IEEE Commun. Surveys Tut.*, vol. 17, no. 1, pp. 315–333, Firstquarter 2015.
- [4] D. Castanheira, R. Magueta, P. Pedrosa, A. Silva, R. Dinis, and A. M. Gameiro, "Hybrid multiuser equalizer with nonlinearity compensation for wideband mmWave massive MIMO uplink systems," *IEEE Trans. Wireless Commun.*, vol. 21, no. 12, pp. 10286–10299, Dec. 2022.
- [5] J. He et al., "A unified power amplifier representation-based receiver equalization technique for nonlinear OFDM signal detection," *IEEE Trans. Commun.*, vol. 72, no. 4, pp. 2260–2274, Apr. 2024.
- [6] Y. Zhang, B. Li, N. Wu, Y. Ma, W. Yuan, and L. Hanzo, "Message passing-aided joint data detection and estimation of nonlinear satellite channels," *IEEE Trans. Veh. Technol.*, vol. 72, no. 2, pp. 1763–1774, Feb. 2023.
- [7] L. Xu, F. Gao, W. Zhang, and S. Ma, "Model aided deep learning based MIMO OFDM receiver with nonlinear power amplifiers," in *Proc. IEEE Wireless Commun. Netw. Conf.*, Nanjing, China, Mar. 2021, pp. 1–6.
- [8] D. Gao et al., "Signal detection in MIMO systems with hardware imperfections: Message passing on neural networks," *IEEE Trans. Wireless Commun.*, vol. 23, no. 1, pp. 820–834, Jan. 2024.
- [9] M. B. Salman and G. M. Guvensen, "An efficient QAM detector via nonlinear post-distortion based on FDE bank under PA impairments," *IEEE Trans. Commun.*, vol. 69, no. 10, pp. 7108–7120, Oct. 2021.
- [10] S. S. Mosleh, L. Liu, C. Sahin, Y. R. Zheng, and Y. Yi, "Brain-inspired wireless communications: Where reservoir computing meets MIMO-OFDM," *IEEE Trans. Neural Netw. Learn. Syst.*, vol. 29, no. 10, pp. 4694–4708, Oct. 2018.
- [11] X. Ma and Z. Gao, "Data-driven deep learning to design pilot and channel estimator for massive MIMO," *IEEE Trans. Veh. Technol.*, vol. 69, no. 5, pp. 5677–5682, May 2020.
- [12] P. Goyal et al., "Accurate, large minibatch SGD: Training ImageNet in 1 hour," Jun. 2017, *arXiv:1706.02677*.
- [13] D. P. Kingma and J. Ba, "Adam: A method for stochastic optimization," in *Proc. Int. Conf. Learn. Representations*, San Diego, CA, USA, May 2015.
- [14] C. Finn, P. Abbeel, and S. Levine, "Model-agnostic meta-learning for fast adaptation of deep networks," in *Proc. Int. Conf. Mach. Learn.*, Sydney, NSW, Australia, Aug. 2017, vol. 70, pp. 1126–1135.
- [15] E. Zedini, A. Kamoun, and M.-S. Alouini, "Performance of multi-beam very high throughput satellite systems based on FSO feeder links with HPA nonlinearity," *IEEE Trans. Wireless Commun.*, vol. 19, no. 9, pp. 5908–5923, Sep. 2020.
- [16] S. Park, H. Jang, O. Simeone, and J. Kang, "Learning to demodulate from few pilots via offline and online meta-learning," *IEEE Trans. Signal Process.*, vol. 69, pp. 226–239, 2021.
- [17] A. Nichol, J. Achiam, and J. Schulman, "On first-order meta-learning algorithms," Oct. 2018, *arXiv:1803.02999*.
- [18] Z. Liu, D. He, N. Wu, Q. Yan, and Y. Li, "Model-driven IEP-GNN framework for MIMO detection with Bayesian optimization," *IEEE Wireless Commun. Lett.*, vol. 13, no. 2, pp. 387–391, Feb. 2024.
- [19] Z. Liu, N. Wu, D. He, W. Yuan, Y. Li, and T. Q. S. Quek, "GNN-Assisted BiG-AMP: Joint channel estimation and data detection for massive MIMO receiver," *IEEE Trans. Wireless Commun.*, vol. 24, no. 6, pp. 4631–4646, Jun. 2025.